

# Is graphene in vacuum an insulator?

Joaquín E. Drut<sup>1</sup> and Timo A. Lähde<sup>2</sup>

<sup>1</sup>*Department of Physics, The Ohio State University, Columbus, OH 43210-1117, USA and*

<sup>2</sup>*Department of Physics, University of Washington, Seattle, WA 98195-1560, USA*

(Dated: November 3, 2018)

We present evidence, from Lattice Monte Carlo simulations of the phase diagram of graphene as a function of the Coulomb coupling between quasiparticles, that graphene in vacuum is likely to be an insulator. We find a semimetal-insulator transition at  $\alpha_g^{\text{crit}} = 1.11 \pm 0.06$ , where  $\alpha_g \simeq 2.16$  in vacuum, and  $\alpha_g \simeq 0.79$  on a SiO<sub>2</sub> substrate. Our analysis uses the logarithmic derivative of the order parameter, supplemented by an equation of state. The insulating phase disappears above a critical number of four-component fermion flavors  $4 < N_f^{\text{crit}} < 6$ . Our data are consistent with a second-order transition.

PACS numbers: 73.63.Bd, 71.30.+h, 05.10.Ln

Graphene, a carbon allotrope with a two-dimensional honeycomb structure, has become an important player at the forefront of condensed matter physics, drawing the attention of theorists and experimentalists alike due to its challenging nature as a many-body problem, its unusual electronic properties and possible technological applications (see Refs. [1, 2] and references therein). Graphene also belongs to a large class of planar condensed-matter systems, which includes other graphite-related materials as well as high- $T_c$  superconductors.

A distinctive feature of graphene is that its band structure contains two degenerate ‘Dirac points’, in the vicinity of which the dispersion is linear, as in relativistic theories [3]. The low-energy excitations in graphene are thus Dirac quasiparticles of Fermi velocity  $v \simeq c/300$ , where  $c$  is the speed of light in vacuum. These are described by the Euclidean action

$$S_E = - \sum_{a=1}^{N_f} \int d^2x dt \bar{\psi}_a D[A_0] \psi_a + \frac{1}{2g^2} \int d^3x dt (\partial_i A_0)^2, \quad (1)$$

where  $g^2 = e^2/\epsilon_0$  for graphene in vacuum,  $\psi_a$  is a four-component Dirac field in 2+1 dimensions,  $A_0$  is a Coulomb field in 3+1 dimensions,  $N_f = 2$  for real graphene, and

$$D[A_0] = \gamma_0(\partial_0 + iA_0) + v\gamma_i\partial_i, \quad i = 1, 2 \quad (2)$$

where the Dirac matrices  $\gamma_\mu$  satisfy the Euclidean Clifford algebra  $\{\gamma_\mu, \gamma_\nu\} = 2\delta_{\mu\nu}$ . The strength of the Coulomb interaction is controlled (as can be shown by rescaling  $t$  and  $A_0$ ) by  $\alpha_g = e^2/(4\pi v\epsilon_0)$ , which is the graphene analogue of the fine-structure constant  $\alpha \simeq 1/137$  of quantum electrodynamics (QED).

Despite the similarities with QED, the smallness of  $v/c$  in graphene has non-trivial consequences: Coulomb interactions between the quasiparticles are essentially instantaneous, thus breaking relativistic invariance which is reflected in Eq. (1). The analogue of the fine-structure constant  $\alpha_g \simeq 300\alpha$  in graphene, such that the low-energy

properties resemble QED in a very strongly coupled regime. This provides an exciting opportunity for the study of strongly coupled theories, within a condensed-matter analogue that can be experimentally realized with modest equipment.

Notably, Eq. (1) satisfies a chiral  $U(2N_f)$  symmetry which can break spontaneously at large enough Coulomb coupling, generating a gap in the quasiparticle spectrum. Whether such an effect occurs in real graphene is an open issue from the experimental point of view (see however Ref. [4], where a substrate-induced gap is reported). On the theoretical side, dynamical gap generation is described by a quantum phase transition due to the formation of particle-hole bound states. However, in such a strongly coupled regime, even a qualitative analysis should be non-perturbative. This is especially true for graphene in vacuum, where  $\alpha_g$  attains its maximum value, while it is partially screened in the presence of a substrate. While the semimetallic properties of graphene on a substrate are well established, the issue of whether a transition to an insulating phase occurs in the absence of a substrate remains unsettled.

This problem has been studied using perturbative as well as non-perturbative methods [5, 6, 7, 8]. The latter, which are typically based on a gap equation, yield an infinite-order transition to an insulating phase above a critical coupling. On the other hand, the results of large- $N_f$  analyses [5, 9, 10] find that Coulomb interactions flow towards a non-interacting fixed point under renormalization-group (RG) transformations, being therefore unable to induce a transition. However, a number of uncontrolled approximations are involved, such as the reliance on large- $N_f$  results that may break down for small  $N_f$ , various approximate treatments of the gap equation kernel, as well as the linearization of the resulting integral equation (see Appendix B of Ref. [8]).

We set out to characterize the phase diagram of graphene in a controlled fashion, which entails a lattice Monte Carlo approach and analysis of the chiral condensate, which is the order parameter for a transition into an

insulating charge-density-wave phase. Such an approach is non-perturbative, takes full account of quantum fluctuations, and has been extensively used [11, 12, 13, 14] in the study of 2+1 (QED<sub>3</sub>) and 3+1 (QED<sub>4</sub>) dimensional QED, but not for studies of graphene (see however Ref. [15], where a model for the strong-coupling limit is investigated).

To this end, we discretize the pure gauge part of Eq. (1) according to (for a recent overview, see Ref. [16])

$$S_E^g[\theta_0] = \frac{\beta}{2} \sum_{\mathbf{n}} \left[ \sum_{i=1}^3 \left( \theta_{0,\mathbf{n}} - \theta_{0,\mathbf{n}+\mathbf{e}_i} \right)^2 \right], \quad (3)$$

where the (dimensionless) lattice coupling  $\beta \equiv v/g^2$ ,  $\theta_0$  is the lattice gauge potential,  $\mathbf{n} \equiv (n_0, \dots, n_3)$  denotes a site on the space-time lattice, and  $\mathbf{e}_\mu$  is a unit vector in the direction  $\mu$ . For studies of chiral phase transitions, staggered fermions [17] are a preferred choice, since chiral symmetry is then partially preserved. As  $N$  staggered flavors correspond to  $N_f = 2N$  continuum Dirac flavors [18], it suffices (for real graphene) to set  $N = 1$ , which gives

$$S_E^f[\bar{\chi}, \chi, U_0] = - \sum_{\mathbf{m}, \mathbf{n}} \bar{\chi}_{\mathbf{m}} D_{\mathbf{m}, \mathbf{n}}[U_0] \chi_{\mathbf{n}}, \quad (4)$$

where the  $\chi_{\mathbf{n}}$  are staggered fermion spinors, and  $(\mathbf{m}, \mathbf{n})$  are restricted to a 2+1 dimensional sublattice. The invariance of Eq. (1) under spatially uniform, time-dependent gauge transformations is retained by coupling the fermions to the gauge field via  $U_0 = \exp(i\theta_0)$ . The staggered form of  $D$  is

$$D_{\mathbf{m}, \mathbf{n}}[U_0] = \frac{1}{2} \left[ \delta_{\mathbf{m}+\mathbf{e}_0, \mathbf{n}} U_{0, \mathbf{m}} - \delta_{\mathbf{m}-\mathbf{e}_0, \mathbf{n}} U_{0, \mathbf{n}}^\dagger \right] + \frac{1}{2} \sum_i \eta_{i, \mathbf{m}} \left[ \delta_{\mathbf{m}+\mathbf{e}_i, \mathbf{n}} - \delta_{\mathbf{m}-\mathbf{e}_i, \mathbf{n}} \right] + m_0 \delta_{\mathbf{m}, \mathbf{n}} \quad (5)$$

where  $\eta_{1, \mathbf{n}} = (-1)^{n_0}$  and  $\eta_{2, \mathbf{n}} = (-1)^{n_0+n_1}$ . The mass term breaks chiral symmetry explicitly, generating a non-zero condensate which is otherwise not possible at finite volume. Extrapolation to  $m_0 = 0$  is thus required. Upon integration of the fermionic degrees of freedom, the path integral is governed by the effective action

$$S_{\text{eff}}[\theta_0] = -N \ln \det(D_{\mathbf{m}, \mathbf{n}}[U_0]) + S_E^g[\theta_0], \quad (6)$$

such that  $P[\theta_0] \equiv \exp(-S_{\text{eff}}[\theta_0])$  defines the Monte Carlo probability measure. It is straightforward to show that the determinant is positive definite. We have sampled  $P[\theta_0]$  using the Metropolis algorithm, updating  $\theta_0$  at random locations and evaluating the fermion determinant exactly. Our approach has been tested against known results for QED<sub>3</sub> and QED<sub>4</sub>. The data of Ref. [11] on the chiral condensate of QED<sub>3</sub> have been accurately reproduced for multiple values of  $N_f$ , along with several randomly chosen datapoints from Refs. [12, 14].

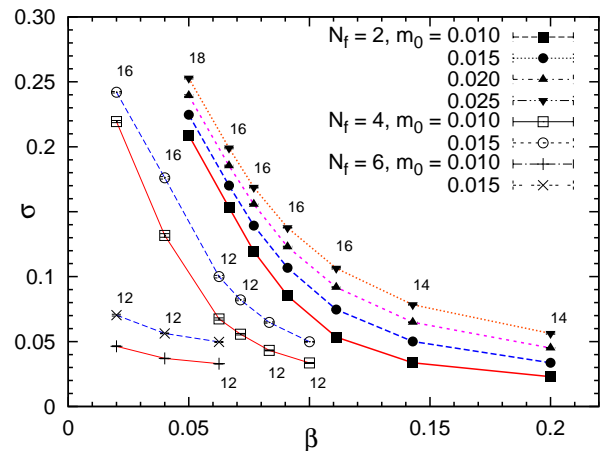


FIG. 1: (Color online) Chiral condensate  $\sigma$  for  $N_f = 2, 4, 6$  as a function of  $\beta$  and  $m_0$ , with lines intended to guide the eye. The lattices are of extent  $L^3 \times L_z$ , such that the fermions live in a 2+1 dimensional cube of size  $L$ , while the gauge bosons also propagate in the  $z$ -direction of length  $L_z$ . For each  $\beta$ , the value of  $L$  is given next to the datapoints. All results are for  $L_z = 8$ , as larger values had no discernible effects. For each datapoint  $\sim 300$  uncorrelated gauge configurations were generated. The statistical uncertainties, which are comparable to the size of the symbols, were obtained by the jackknife method [24]. Finite volume effects are largest for small  $\beta$ .

The chiral  $U(2N_f)$  symmetry of the continuum theory can only partially be realized on the lattice if the doubling problem is to be avoided [19]. In particular, only a global  $U(N) \times U(N)$  symmetry remains upon discretization [18]. We focus on the spontaneous breakdown of this symmetry to a  $U(N)$  subgroup, characterized by a condensate  $\sigma \equiv \langle \bar{\chi} \chi \rangle \neq 0$  in the limit  $m_0 \rightarrow 0$ , which marks the appearance of a gap in the quasiparticle spectrum. Our results for  $\sigma$  are presented in Fig. 1 for  $\beta = 0.05, \dots, 0.5$  and  $m_0 = 0.010, \dots, 0.025$  (in lattice units).

Our data for  $N_f = 2$  in Fig. 1 are suggestive of a critical coupling  $\beta_c \sim 0.06 \dots 0.09$ , below which  $\sigma$  survives in the limit  $m_0 \rightarrow 0$ . More significantly, the susceptibility  $\chi_l = \partial \sigma / \partial m_0$  shown in the right panel of Fig. 2 exhibits a maximum which tends towards  $\beta_c$  as  $m_0$  is decreased. The (much more limited) data for  $N_f = 4$  (not shown) have a similar maximum around  $\beta \sim 0.03$ . As  $N_f$  is increased,  $\sigma$  obviously becomes suppressed, vanishing between  $N_f = 4$  and  $N_f = 6$ . This agrees with large- $N_f$  results [10] that yield a quantum critical point (and therefore no condensate) in the limit  $\beta \rightarrow 0$ , and is consistent with recent Monte Carlo studies of that limit [15]. Our results for small  $N_f$  establish that the strong-coupling critical point disappears below  $N_f^{\text{crit}}$ , with  $4 < N_f^{\text{crit}} < 6$ .

For a quantitative determination of  $\beta_c$ , we compute the logarithmic derivative  $R$  of  $\sigma$  with respect to  $m_0$ ,

$$R \equiv \left. \frac{\partial \ln \sigma}{\partial \ln m_0} \right|_{\beta} = \frac{m_0}{\sigma} \left( \left. \frac{\partial \sigma}{\partial m_0} \right) \right|_{\beta}, \quad (7)$$

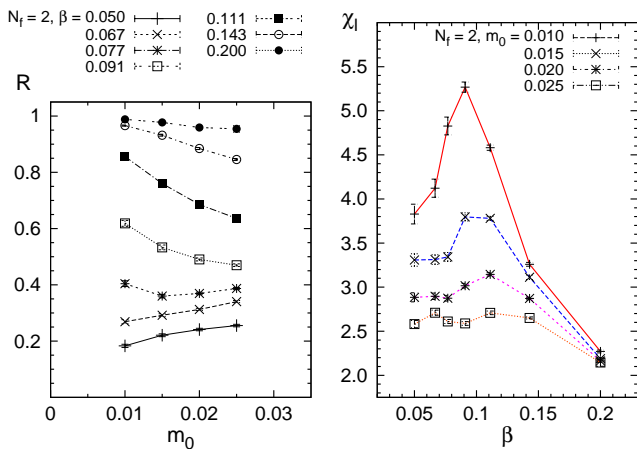


FIG. 2: (Color online) Left panel: Logarithmic derivative  $R$  as a function of  $m_0$  for different  $\beta$ . Right panel: Chiral susceptibility  $\chi_l$  as a function of  $\beta$  for different  $m_0$ . All data are for  $N_f = 2$ , with lattice sizes identical to those of Fig. 1. The lines are intended as a guide to the eye.

according to the method of Ref. [20]. In the limit  $m_0 \rightarrow 0$ , the behavior of  $R$  is as follows:  $R \rightarrow 1$  in the chirally symmetric (unbroken) phase, where  $\sigma \propto m_0$ . At the critical coupling  $\beta = \beta_c$  one finds that  $R \rightarrow 1/\delta$ , where  $\delta$  is a universal critical exponent.  $R$  vanishes in the spontaneously broken phase, where  $\sigma \neq 0$  for  $m_0 \rightarrow 0$ . The data in Fig. 2 (left panel) indicate that chiral symmetry is spontaneously broken for  $\beta = 0.067$ , but remains unbroken for  $\beta = 0.077$ , from which we conclude that  $\beta_c = 0.072 \pm 0.005$ . This estimate can be refined by use of larger lattice volumes and smaller values of  $m_0$ .

A more precise determination of  $\beta_c$  requires an equation of state (EOS) of the form  $m_0 = f(\sigma, \beta)$  for the extrapolation  $m_0 \rightarrow 0$ . We have considered the EOS successfully applied [12, 13] to QED<sub>4</sub>,

$$m_0 X(\beta) = Y(\beta) f_1(\sigma) + f_3(\sigma), \quad (8)$$

where  $X(\beta)$  and  $Y(\beta)$  are expanded around  $\beta_c$  such that  $X(\beta) = X_0 + X_1(1 - \beta/\beta_c)$  and  $Y(\beta) = Y_1(1 - \beta/\beta_c)$ . The dependence on  $\sigma$  is given by  $f_1(\sigma) = \sigma^b$  and  $f_3(\sigma) = \sigma^\delta$ , which allows for non-classical critical exponents  $\delta$  and  $\beta$  [12, 13], where  $b \equiv \delta - 1/\beta$ . A  $\chi^2$  fit of Eq. (8) to the data in Fig. 1 is given in Fig. 3 (left panel), along with a ‘‘Fisher plot’’ of  $\sigma^2$  versus  $m_0/\sigma$  (right panel). Deviations from classical mean-field behavior manifest themselves in the Fisher plot as curvature in the lines of constant  $\beta$ . The mostly straight lines in Fig. 3 (right panel) indicate that the data should be well described, up to finite-size effects, by the classical values  $\delta = 3$  and  $b = 1$ , which is confirmed in Fig. 3 (left panel).

For all values of  $m_0$ , the finite-volume effects appear to be dominated by a dynamically generated correlation length in the region that we identify as the spontaneously broken phase. To gauge the impact of such effects on  $\beta_c$ ,

several fits were performed from  $L = 8$  up to the main fit with  $L = 16$ . Our analysis indicates that  $\beta_c$  is stable around  $\sim 0.075$ , even though the datapoints at the smallest  $\beta$  shift due to finite-volume effects. In contrast, for  $N_f = 6$  chiral symmetry remains unbroken, and thus finite-volume effects remain small in the limit  $\beta \rightarrow 0$ . The stability of  $\beta_c$  can be understood in terms of the results for  $R$  in Fig. 2, since any fit to the condensate should be consistent with the susceptibility as well, and  $R$  combines both pieces of information. The character of  $R$  clearly changes around  $\beta = 0.075$ , in direct correlation with the fitted values of  $\beta_c$ . If one allows for extreme modifications, such as non-classical critical exponents, or forces the fit to account for all the datapoints, values of  $\beta_c$  as low as 0.060 may be found, although at the price of a much worse fit to the data. By inclusion and exclusion of different sets of datapoints, a realistic (though somewhat model-dependent) estimate of the critical coupling is  $\beta_c = 0.0755 \pm 0.0008$ . Possible deviations from classical mean-field behavior with  $f_1 = \sigma$  and  $f_3 = \sigma^3$  are below the resolution of the present study.

The results in Fig. 3 suggest a second-order transition with classical exponents, unlike Refs. [6, 8], where an infinite-order transition was found. In this situation, further investigation is clearly called for. While the sensitivity of our analysis increases for smaller  $m_0$ , larger lattice volumes are also required to keep finite-volume effects under control. A similar EOS analysis has recently been performed by Hands and Strouthos (Ref. [15]) for a

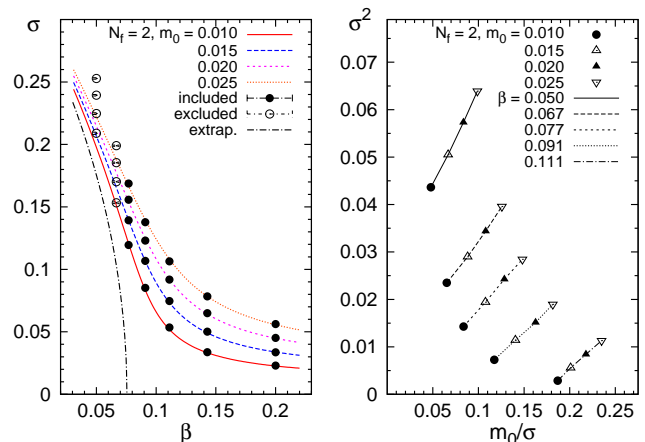


FIG. 3: (Color online) Left panel:  $\chi^2$  fit to the data of Fig. 1 and extrapolation to  $m_0 = 0$  for  $N_f = 2$  using Eq. (8) with  $X_0, X_1, Y_1$  and  $\beta_c$  as free parameters. The points with largest finite-volume effects have been excluded from the fit. The optimal parameter values are  $\beta_c = 0.0755 \pm 0.0003$ ,  $X_0 = 0.195 \pm 0.003$ ,  $X_1 = -0.089 \pm 0.001$  and  $Y_1 = -0.091 \pm 0.001$ . The uncertainties are purely statistical. Right panel: Fisher plot of  $\sigma^2$  versus  $m_0/\sigma$  for the data of Fig. 1 with  $N_f = 2$ . The lines connect datapoints with identical  $\beta$ , such that straight lines indicate mean-field behavior according to Eq. (8). At  $\beta_c$ , the extrapolation crosses the origin.

graphene-like theory with a zero-range interaction. Unfortunately, a meaningful comparison is not possible at this time, as their parameter  $1/g^2$  cannot be identified with our gauge coupling  $\beta$ , except in the strong-coupling limit  $\beta \rightarrow 0$ .

A comparison with experiment necessitates a discussion of renormalized quantities. While test charges remain unscreened as the fluctuations of the fermion action are confined to  $2 + 1$  dimensions, the physical value of  $\beta_c$  may be affected by renormalization of  $v$  due to the breaking of relativistic invariance. Large- $N_f$  results suggest [5, 10] that the Coulomb interaction renormalizes  $v$  logarithmically toward larger values, thereby decreasing  $\alpha_g$  slightly from the bare value, and strengthening our conclusions for graphene in vacuum. Available experimental evidence [4, 6] indicates that velocity renormalization is at most a  $\sim 20\%$  effect, and of phononic rather than Coulombic origin.

Summarizing, we have found that graphene should become insulating at a critical coupling  $\alpha_g^{\text{crit}} \equiv 1/(4\pi\beta_c) = 1.11 \pm 0.06$ , where  $\beta_c = 0.072 \pm 0.005$ . This should be compared with  $\alpha_g \simeq 2.16$  in vacuum, and  $\alpha_g \simeq 0.79$  on an  $\text{SiO}_2$  substrate (using the experimental value  $v \simeq 10^6$  m/s). These findings are in line with the observed semimetallic properties [1] of graphene on a  $\text{SiO}_2$  substrate, and predict that the Coulomb interaction in suspended graphene should induce a gap in the quasiparticle spectrum. Within the accuracy of the present study, the transition appears to be of second order.

Ultimately, the observation of the insulating phase is dependent on the size of the induced band gap. However, the prediction of a dimensionful observable requires the matching of a lattice quantity (other than the gap itself) to the corresponding experimental value. This applies to finite temperature studies as well, where it is necessary to fix the absolute temperature scale. An intriguing possibility is that the observed nanoscale ripples in suspended graphene [21] may provide the necessary information, as such corrugations can be described [22] by means of external gauge fields with known dimensionful properties. Exploratory work in this direction, along with a more accurate study of the transition properties, is in progress [23].

We acknowledge support under U.S. DOE Grants No. DE-FG-02-97ER41014, No. DE-FG02-00ER41132, and No. DE-AC02-05CH11231, UNEDF SciDAC Collaboration Grant No. DE-FC02-07ER41457 and NSF Grant No. PHY-0653312. This work was supported in part by an allocation of computing time from the Ohio Supercomputer Center. We thank A. Bulgac and M. J. Sav-

age for computer time, and W. Detmold, M. M. Forbes, R. J. Furnstahl, D. Gazit and D. T. Son for instructive discussions.

- 
- [1] K. S. Novoselov, *Science* **306**, 666 (2004); K. S. Novoselov *et al.*, *Proc. Natl. Acad. Sci. U.S.A.* **102**, 10451 (2005); *Nature (London)* **438**, 197 (2005); A. K. Geim, K. S. Novoselov, *Nat. Mat.* **6**, 183 (2007).
  - [2] A. H. Castro Neto *et al.*, *Phys. Mod. Phys.* (to be published), [arXiv:0709.1163].
  - [3] G. W. Semenoff, *Phys. Rev. Lett.* **53**, 2449 (1984).
  - [4] S. Y. Zhou *et al.*, *Nat. Mater.* **6**, 770 (2007); *ibid.* **7**, 259 (2008); *ibid.* *Physica E* **40**, 2642 (2008); A. Bostwick *et al.*, *Nature Phys.* **3**, 36 (2007); G. Li, A. Luican, E. Andrei, [arXiv:0803.4016].
  - [5] J. González, F. Guinea, M. A. H. Vozmediano, *Nucl. Phys. B* **424**, 595 (1994); *Phys. Rev. Lett.* **77**, 3589 (1996); *Phys. Rev. B* **59**, R2474 (1999); O. Vafek, M. J. Case, *ibid.* **77**, 033410 (2008).
  - [6] D. V. Khvashchenko, *Phys. Rev. Lett.* **87**, 246802 (2001); [arXiv:0807.0676]; H. Leal, D. V. Khvashchenko, *Nucl. Phys. B* **687**, 323 (2004);
  - [7] A. L. Tchougreeff, R. Hoffmann, *J. Phys. Chem.* **96**, 8993 (1992); F. R. Wagner, M.-B. Lepetit, *ibid.* **100**, 11050 (1996).
  - [8] E. V. Gorbar *et al.*, *Phys. Rev. B* **66**, 045108 (2002).
  - [9] I. F. Herbut, *Phys. Rev. Lett.* **97**, 146401 (2006).
  - [10] D. T. Son, *Phys. Rev. B* **75**, 235423 (2007).
  - [11] J. B. Kogut, E. Dagotto, A. Kocić, *Phys. Rev. Lett.* **60**, 772 (1988); *ibid.* **62**, 1083 (1989).
  - [12] M. Göckeler *et al.*, *Nucl. Phys. B* **334**, 527 (1990); *ibid.* **371**, 713 (1992); *ibid.* **487**, 313 (1997).
  - [13] A. A. Khan, *Phys. Rev. D* **53**, 6416 (1996).
  - [14] S. J. Hands, J. B. Kogut, C. G. Strouthos, *Nucl. Phys. B* **645**, 321 (2002).
  - [15] S. J. Hands, C. G. Strouthos, *Phys. Rev. B* **78**, 165423 (2008).
  - [16] H. J. Rothe, “Lattice Gauge Theories - an Introduction”, 3<sup>rd</sup> edition, World Scientific, Singapore (2005).
  - [17] J. Kogut, L. Susskind, *Phys. Rev. D* **11**, 395 (1975); L. Susskind, *ibid.* **16**, 3031 (1977); H. Kluberg-Stern, *Nucl. Phys. B* **220**, 447 (1983).
  - [18] C. Burden, A. N. Burkitt, *Eur. Phys. Lett.* **3**, 545 (1987).
  - [19] H. B. Nielsen, M. Ninomiya, *Nucl. Phys. B* **185**, 20 (1981) [Erratum *ibid.* **195**, 541 (1982)]; *ibid.* **193**, 173 (1981).
  - [20] A. Kocić, J. B. Kogut, K. C. Wang, *Nucl. Phys. B* **398**, 405 (1993).
  - [21] J. C. Meyer *et al.*, *Nature (London)* **446**, 60 (2007).
  - [22] F. Guinea, B. Horovitz, P. Le Doussal, *Phys. Rev. B* **77**, 205421 (2008).
  - [23] J. E. Drut, T. A. Lähde, [arXiv:0901.0584].
  - [24] M. C. K. Yang, D. H. Robinson, “Understanding and learning science by computer”, Series in Computer Science, Vol. 4, World Scientific (1986).